

Expression and Stereochemical and Isotope Effect Studies of Active 4-Oxalocrotonate Decarboxylase[†]

Thanuja M. Stanley, William H. Johnson Jr., Elizabeth A. Burks, and Christian P. Whitman*

Medicinal Chemistry Division, College of Pharmacy, The University of Texas, Austin, Texas 78712-1071

Chi-Ching Hwang and Paul F. Cook*

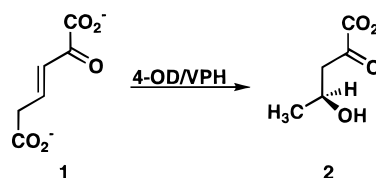
Department of Chemistry and Biochemistry, University of Oklahoma, 620 Parrington Oval, Norman, Oklahoma 73019-9425

Received August 12, 1999; Revised Manuscript Received November 11, 1999

ABSTRACT: 4-Oxalocrotonate decarboxylase (4-OD) and vinylpyruvate hydratase (VPH) from *Pseudomonas putida* mt-2 form a complex that converts 2-oxo-3-hexenedioate to 2-oxo-4-hydroxypentanoate in the catechol meta fission pathway. To facilitate mechanistic and structural studies of the complex, the two enzymes have been coexpressed and the complex has been purified to homogeneity. In addition, Glu-106, a potential catalytic residue in VPH, has been changed to glutamine, and the resulting E106QVPH mutant has been coexpressed with 4-OD and purified to homogeneity. The 4-OD/E106QVPH complex retains full decarboxylase activity, with comparable kinetic parameters to those observed for 4-OD in the wild-type complex, but is devoid of any detectable hydratase activity. Decarboxylation of (5*S*)-2-oxo-3-[5-D]hexenedioate by either the 4-OD/VPH complex or the mutant complex generates 2-hydroxy-2,4*E*-[5-D]pentadienoate in D₂O. Ketonization of 2-hydroxy-2,4-pentadienoate by the wild-type complex is highly stereoselective and results in the formation of 2-oxo-(3*S*)-[3-D]-4-pentenoate, while the mutant complex generates a racemic mixture. These results indicate that 2-hydroxy-2,4-pentadienoate is the product of 4-OD and that 2-oxo-4-pentenoate results from a VPH-catalyzed process. On this basis, the previously proposed hypothesis for the conversion of 2-oxo-3-hexenedioate to 2-oxo-4-hydroxypentanoate has been revised [Lian, H., and Whitman, C. P. (1994) *J. Am. Chem. Soc.* 116, 10403–10411]. Finally, the observed ¹³C kinetic isotope effect on the decarboxylation of 2-oxo-3-hexenedioate by the 4-OD/VPH complex suggests that the decarboxylation step is nearly rate-limiting. Because the value is not sensitive to either magnesium or manganese, it is likely that the transition state for carbon–carbon bond cleavage is late and that the metal positions the substrate and polarizes the carbonyl group, analogous to its role in oxalacetate decarboxylase.

4-Oxalocrotonate decarboxylase (EC 4.1.1.-; 4-OD)¹ and vinylpyruvate hydratase (EC 4.2.1.-; VPH) from *Pseudomonas putida* mt-2 catalyze two successive reactions in the catechol meta fission pathway, which result in the conversion of 2-oxo-3-hexenedioate (**1**) to 2-oxo-4*S*-hydroxypentanoate (**2**, Scheme 1) (1–3). The two enzymes form a complex and utilize either manganese or magnesium as a cofactor (1, 2). The enzymes are expressed by separate genes and are part of an inducible pathway encoded by the TOL plasmid pWW0 (2). The entire pathway enables certain strains of soil bacteria to use compounds such as toluene, *m*- and *p*-xylene,

Scheme 1



3-ethyltoluene, and 1,2,4-trimethylbenzene as their sole sources of carbon and energy (3).

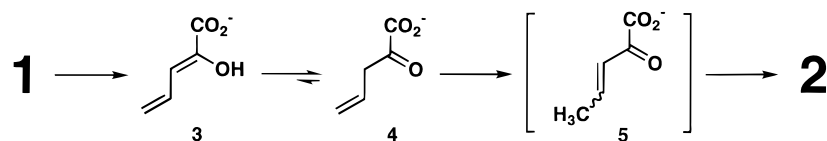
Our previous studies on the 4-OD/VPH complex suggested that 4-OD catalyzes the decarboxylation of **1** to 2-oxo-4-pentenoate (**4**) through the intermediate 2-hydroxy-2,4-pentadienoate (**3**, Scheme 2) (4). The subsequent transformation of **4** to **2** could reasonably involve the allylic isomerization of **4** to **5** followed by the Michael addition of water to **5**. The working hypothesis for 4-OD was based, in part, on the analogous metal-dependent decarboxylation of oxalacetate (**6**, Scheme 3) catalyzed by oxalacetate decarboxylase (OAD) (5). The only difference between **1** and **6** is the presence of the double bond in **1** so that decarboxylation generates the vinylogous analogue of enolpyruvate (**7**). This working hypothesis was further supported by the

[†] This research was supported by the National Institutes of Health to C.P.W. (GM-41239) and P.F.C. (GM 36799).

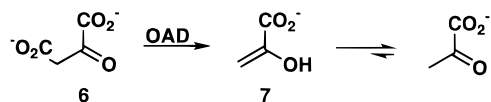
* Address correspondence to either author. C.P.W.: Tel 512-471-6198; Fax 512-232-2606; E-mail cwhitman@uts.cc.utexas.edu. P.F.C.: Tel 405-325-4581; Fax 405-325-7182; E-mail pcook@chemdept.chem.ou.edu.

¹ Abbreviations: BCA, bicinechonic acid; DEAE, diethylaminoethyl; HPLC, high-performance liquid chromatography; IPTG, isopropyl β-D-thiogalactoside; Kn, kanamycin; LB, Luria–Bertani medium; NMR, nuclear magnetic resonance; 4-OT, 4-oxalocrotonate tautomerase; 4-OD, 4-oxalocrotonate decarboxylase; SDS–PAGE, sodium dodecyl sulfate–polyacrylamide gel electrophoresis; VPH, vinylpyruvate hydratase.

Scheme 2



Scheme 3



following observations. In the absence of the divalent metal ion, the formation of **2** from **1** slowed considerably and both **3** and **4** accumulated (**4**). The accumulation of these intermediates is particularly pronounced in D_2O . Thus, it appeared that the decarboxylation reaction was uncoupled from the hydration reaction. Under these conditions, (3*S*)-[3- D]**4** was generated from **3**, in D_2O , nearly stereospecifically (**4**). This result implicated **4** as the product of the decarboxylation reaction and as the substrate for the hydration reaction.

Part of our proposed mechanism for 4-OD relies on the inference that the absence of the metal ion uncouples the two reactions. To determine whether this supposition is valid and to study each individual reaction further, two strategies were pursued that would clearly separate the decarboxylation and the hydration reactions. In the first strategy, the two enzymes were separately cloned and expressed. Unfortunately, the instability of the partially purified 4-OD and the insolubility of VPH led us to abandon this approach.

In an alternative approach, an expression vector for the 4-OD/VPH complex was constructed and sequence analysis was used to identify conserved and potential catalytic residues in VPH (6, 7). Site-directed mutagenesis of one of these residues, Glu-106, to a glutamine resulted in the expression of a complex that fully retained decarboxylase activity but was devoid of hydratase activity. A stereochemical study revealed that the 4-OD/E106QVPH complex generated a racemic mixture of [3- D]**4** upon its incubation with **3** in D_2O , indicating that **4** results from a nonenzymatic process and that the previously observed stereospecific incorporation of a deuterium at C-3 of **4** must result from the VPH-catalyzed reaction. Subsequently, the decarboxylation reaction in the 4-OD/VPH complex was explored by measuring ^{13}C isotope effects for both the enzymatic and nonenzymatic reactions in order to determine the role of the metal ion in the mechanism and whether the double bond affects the mechanism. Our findings provide new insights into the mechanism of 4-OD and result in a revision of the sequence of events leading from **1** to **2**.

EXPERIMENTAL PROCEDURES

Materials. Tryptone, yeast extract, and agar were obtained from Difco (Detroit, MI). Restriction enzymes, T4 DNA ligase, PCR reagents (with the exceptions noted below), and the Wizard DNA mini- and maxiprep kits were obtained from Promega (Madison, WI). The deoxynucleotide triphosphates were purchased from Boehringer-Mannheim (Indianapolis, IN). The *Pfu* DNA polymerase and its 10 \times buffer were purchased from Stratagene (La Jolla, CA). The pET-24a(+)

plasmid was obtained from Novagen (Madison, WI). T7 promoter and terminator oligonucleotide primers as well as primers for DNA amplification and sequencing were synthesized by either Genosys (The Woodlands, TX) or Oligos, Etc. (Wilsonville, OR). The QIAprep spin miniprep kit was obtained from Qiagen (Valencia, CA). The plasmid pG-SH2915 was a gift from Dr. Shigeaki Harayama (Marine Biotechnology Institute, Kamaishi City, Japan). The GeneClean II kit was obtained from Bio 101, Inc. (Vista, CA). Agarose, the 1 kb and 100 bp DNA ladders, the prestained protein molecular weight standards (low range), calf intestinal alkaline phosphatase, electroporation chambers, and the Cell-Porator electroporation system I were purchased from Gibco BRL/Life Technologies, Inc. (Grand Island, NY). Thin-walled PCR tubes and isopropyl β -D-thiogalactoside (IPTG) were obtained from Ambion, Inc. (Austin, TX). The bicinchoninic acid (BCA) protein assay kit was purchased from Pierce (Rockford, IL). The ultrafiltration apparatus and the YM-10 ultrafiltration membranes were acquired from Amicon/Millipore (Bedford, MA). The synthesis of 2-hydroxy-muconate (**8**) and the purification of 4-oxalocrotonate tautomerase (4-OT) are described elsewhere (8, 9). All other biochemicals and buffers were obtained from either Sigma Chemical Co. or Aldrich Chemical Co.

Strains. *Escherichia coli* strain DH5 α was obtained from Gibco BRL/Life Technologies, Inc. and was used for the transformation of ligated plasmids. The *E. coli* strain BL21-(DE3) was obtained from Novagen and was used for the expression of the recombinant proteins. *Pseudomonas putida* mt-2 (ATCC 33015) was obtained from American Type Culture Collection (Rockville, MD) and was used as the source of the TOL plasmid.

General Methods. Techniques for restriction digestions, ligations, plasmid purification, and other standard molecular biology manipulations were based on methods described elsewhere (10). The speed prep technique for plasmid purification was based on a previously published method (11). The colony screening technique using PCR is based on a method described in the pET system manual (Novagen, Inc., sixth edition, August, 1995). The PCR was carried out in a DNA thermal cycler (Model 480) obtained from Perkin-Elmer (Norwalk, CT). DNA sequencing was performed at the DNA Sequencing Facility, University of Texas at Austin (Austin, TX). Protein concentrations were determined with the BCA protein assay kit. Sodium dodecyl sulfate-polyacrylamide gel electrophoresis (SDS-PAGE) was performed under denaturing conditions on 15% gels (0.4% cross-link) (12). High-performance liquid chromatography (HPLC) was performed at 23 $^{\circ}C$ with either a Waters Protein Pak DEAE-5PW anion-exchange column (15 \times 2.15 cm) or a Bio-Rad Bio-Gel phenyl-5-PW hydrophobic interaction column (15 \times 2.15 cm) attached to a Waters system. Kinetic data were obtained at 23 $^{\circ}C$ on either a Hewlett-Packard 8452A diode-array spectrophotometer or a Perkin-Elmer Lambda Bio-10 UV/vis spectrometer. The kinetic data were

fitted by nonlinear regression data analysis with the Grafit program (Erathicus Software Ltd., Staines, U.K.) obtained from Sigma Chemical Co. NMR spectra were acquired on either a Bruker AM-250 or a Varian Unity INOVA-500 spectrometer, as indicated.

Construction of the 4-OD/VPH Expression Vector. A plasmid that coexpressed both 4-OD and VPH was constructed by a method described elsewhere (13). The pET24a-4OD recombinant plasmid was used as the template for the PCR amplification of a fragment containing the 4-OD gene followed by the sites noted below. The construction of the pET24a-4OD recombinant plasmid is described in the Supporting Information. Two oligonucleotide primers, 5'-TAATACGACTCACTATAGG-3' and 5'-CAGATCAGT-CATATGTATATCTCCTTGGATCCCTATCA-GACGAAGCG-3', were synthesized for this purpose. The sequence of the first primer corresponds to the T7 promoter region of pET-24a(+). The second primer contains a *Nde*I restriction site (underlined) followed by the complementary sequence for a TATA box and a ribosomal binding site. A *Bam*HI restriction site (boldface type) was introduced next, followed by the complementary sequence for two stop codons, and nine bases corresponding to the complementary sequence of the *xyI* gene. A 25 μ L reaction mixture was made up as described above. The PCR protocol consisted of 35 cycles, a 2-min incubation period at 94 °C preceding the 35 cycles, and a 5-min incubation period at 72 °C following the 35 cycles. Each cycle consisted of three steps: denaturation at 94 °C for 1 min, annealing at 55 °C for 1 min, and elongation at 72 °C for 2 min. The amplified products were analyzed by electrophoresis on a 1% agarose gel as described elsewhere (14), and extracted from the gel by use of the GeneClean II kit. Both the purified PCR fragment and the pET24a-VPH were treated with *Nde*I restriction enzyme as described (10), purified on a 1% agarose gel, and extracted from the gel (14). The construction of the pET24a-VPH recombinant plasmid is described in the Supporting Information. The linearized pET24a-VPH was then treated with calf intestinal alkaline phosphatase (CIP) as described (10), purified on a 1% agarose gel, and extracted from the gel (14). Subsequently, the digested 4-OD fragment and the dephosphorylated linearized pET24a-VPH vector were ligated as described elsewhere (10). The DNA was precipitated, resuspended in 10 μ L of sterile water, and transformed into *E. coli* DH5 α cells by electroporation. The transformed cells were grown at 37 °C for 2 h and then aliquots (1 mL) were centrifuged (3000 rpm, 3 min). A portion (950 μ L) of the supernatant was removed and the cell pellet was resuspended in the remaining volume. The resulting suspension was spread onto a LB/Kn (100 μ g/mL) plate and grown at 37 °C overnight. One hundred randomly selected colonies were screened for the insert by a PCR multiplex technique described elsewhere (15). A positive colony was grown in liquid LB/Kn (10 mL, 100 μ g/mL) medium at 37 °C overnight, and the newly constructed plasmid (designated pET24a-4OD/VPH) was isolated by use of the QIAprep spin miniprep kit according to the manufacturer's directions.

To verify that the 4-OD insert had been introduced in the correct orientation, the pET24a-4OD/VPH plasmid was treated with restriction enzymes as described (10) and the fragments were analyzed. In one experiment, the plasmid

was treated with *Pst*I and *Hind*III restriction enzymes. In a second separate experiment, the plasmid was treated with *Bam*HI and *Xho*I restriction enzymes. There is a unique *Pst*I restriction site in the recombinant plasmid located at bases 64–69 of the 4-OD gene and a unique *Hind*III restriction site in the pET-24a(+) vector immediately downstream of the *Sal*I restriction site at the 3' end of the VPH gene. Thus, if the 4-OD gene is inserted in the correct orientation, treatment of the plasmid with both restriction enzymes will yield about a fragment of ~1550 base pairs. If the 4-OD gene is inserted in the reverse orientation, a fragment of ~850 base pairs will result. Analysis by gel electrophoresis revealed the presence of the 1550 base pair insert. A unique *Bam*HI restriction site was constructed into the recombinant plasmid between the 4-OD gene and the VPH gene. There are two *Xho*I restriction sites—one is located at bases 529–534 of the 4-OD gene. If the 4-OD gene is inserted in the correct orientation, treatment of the plasmid with both restriction enzymes will yield a fragment of ~800 base pairs. If the 4-OD gene is inserted in the reverse orientation, a fragment of ~1300 base pairs will result. Analysis by gel electrophoresis revealed the presence of the 800 base pair insert. Thus, the plasmid, with 4-OD inserted in the correct orientation, was introduced in *E. coli* lysogen B strain BL21-(DE3) by electroporation as described (14). For sequencing, the plasmid was isolated as described elsewhere (14).

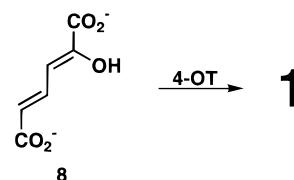
Overexpression and Purification of 4-OD/VPH. The expression strain was grown under the conditions described elsewhere (14). Typically, a 3 L culture yields 5 g of cells. The harvested cells were suspended in chilled 20 mM Tris-HCl, pH 7.3 (2.5 mL/g of cells), containing 5 mM MnCl₂, disrupted by sonication, and centrifuged as described above. The supernatant was purified by a modification of a literature protocol (2). In this modified procedure, the supernatant (10 mL) was loaded in 2-mL aliquots onto a DEAE-5PW anion-exchange column attached to a Waters HPLC column and preequilibrated with 20 mM Tris-HCl buffer, pH 7.3. After a 15 min wash, the 4-OD/VPH was eluted with a linear NaCl gradient (0.0–0.4 M in 60 min) at a flow rate of 5 mL/min. Fractions (10 mL) were collected and assayed for activity. The fractions with the highest activity were pooled and concentrated, and the concentrate was made 1.2 M in (NH₄)₂SO₄. After being stirred for 1 h at 4 °C, the solution was centrifuged (34000g, 30 min). The supernatant was then loaded onto a phenyl-5-PW column and eluted as described (2). Fractions (10 mL) were collected and assayed for activity. Peak fractions were approximately 90% homogeneous as assessed by SDS–PAGE. For additional purity (>95%), the fractions are pooled, concentrated, and loaded onto the DEAE anion-exchange column and eluted as described above. The yield of purified protein is ~30 mg from 5 g of cells. Subsequently, the fractions from the anion-exchange column were loaded onto a Sephadex G-150 column (1 \times 100 cm) equilibrated with 20 mM Tris-HCl buffer (pH 7.3) containing 0.15 M NaCl and 5 mM MnCl₂. Fractions (1 mL) were collected, assayed for activity, and stored at 4 °C.

Site-Directed Mutagenesis. The E106Q mutant VPH was constructed by overlap extension PCR as described elsewhere (16). The external primers were oligonucleotides 5'-TAATACGACTCACTATAGG-3' (designated primer A) and 5'-GCTAGTTATTGCTCAGCGG-3' (designated primer

D). Primer A corresponds to the coding sequence of the T7 promoter region of the pET-24a(+) vector, while primer D corresponds to the complementary sequence of the region upstream from the T7 terminator region of the vector. The internal primers used to construct the E106Q VPH mutant were 5'-GCCCTGGGCGCGCGGCTGGATCAG-3' (primer B) and 5'-CTGATCCAGCCGCGCGCCAGGGC-3' (primer C). In each primer, the mutation is underlined and the remaining bases correspond to the coding sequence (primer C) or the complementary sequence (primer B) for the VPH gene. Each 25 μ L PCR reaction contained primers A and B (1 μ M final concentration each), the dNTPs (0.7 mM final concentration), 10 \times buffer (2.5 μ L), *Pfu* DNA polymerase (1.25 units), and pET24a-4OD/VPH (0.7 μ g) as template. The PCR protocol consisted of 25 cycles, a 1-min incubation period at 94 $^{\circ}$ C preceding the 25 cycles, and a 10-min incubation period at 72 $^{\circ}$ C following the 25 cycles. Each cycle consisted of three steps: denaturation at 94 $^{\circ}$ C for 45 s, annealing at 55 $^{\circ}$ C for 45 s, and elongation at 72 $^{\circ}$ C for 2 min. The amplified products were analyzed by electrophoresis on a 1% agarose gel as described elsewhere (14), and the AB fragment was extracted from the gel by use of the GeneClean II kit. The CD fragment was constructed similarly with two exceptions: the pET24a-VPH (0.43 μ g) was used as the template in the PCR, and the 25 cycles were followed by a 5-min incubation period at 72 $^{\circ}$ C. The AD segment (\sim 1800 base pairs) was constructed with *Taq* DNA polymerase because all attempts with the *Pfu* DNA polymerase were unsuccessful. Thus, each 25 μ L PCR reaction contained primers A and D (1 μ M final concentration each), the dNTPs (0.2 mM final concentration), 10 \times buffer (2.5 μ L), $MgCl_2$ (1.5 mM final concentration), *Taq* DNA polymerase (0.625 unit), and the AB and CD fragments (1 μ L each). The PCR protocol consisted of 25 cycles, a 1-min incubation period at 94 $^{\circ}$ C preceding the 25 cycles, and a 10-min incubation period at 72 $^{\circ}$ C following the 25 cycles. Each cycle consisted of three steps: denaturation at 94 $^{\circ}$ C for 1 min, annealing at 55 $^{\circ}$ C for 1 min, and elongation at 72 $^{\circ}$ C for 2.25 min. The AD fragment was purified as described above. Subsequently, the AD fragment and the pET24a(+) vector were treated with *Xba*I and *Hind*III restriction enzymes as described (10), purified on a 1% agarose gel, and extracted from the gel by use of the GeneClean II kit. Subsequently, the linearized vector and the AD fragment were ligated as described above and the DNA was used to transform *E. coli* strain DH5 α by electroporation as described (10, 14). After the transformed cells were screened for the presence of insert, a colony containing the insert was grown and the newly constructed plasmid (designated pET24a-4-OD/E106QVPH) was isolated and introduced in *E. coli* lysogen B strain BL21(DE3) by electroporation as described (14). The plasmid was isolated and sequenced as described elsewhere (14).

Overexpression and Purification of 4-OD/E106QVPH. The expression strain was grown under the conditions described elsewhere (14). Typically, a 3 L culture yields 4 g of cells. The 4-OD/E106QVPH complex was purified following the procedure used for the purification of the 4-OD/VPH complex. After passage through the phenyl column, 30 mg of protein (\sim 90% homogeneous) is typically obtained from 3 L of culture.

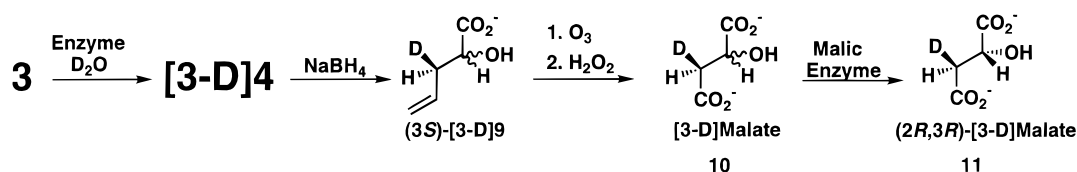
Scheme 4



Enzymatic Assays and Kinetics. 4-OD activity was monitored by following the rate of the disappearance of **1** at 236 nm ($\epsilon = 6580 \text{ M}^{-1} \text{ cm}^{-1}$), which was generated in situ by the incubation of 2-hydroxymuconate (**8**) with 4-OT (Scheme 4) (4). The assay mixture consisted of 20 mM NaH_2PO_4 buffer, pH 7.3, made 5 mM in MgCl_2 (1 mL final volume), varying amounts (1–10 μ L) of **8** from a stock solution (2.0 or 8.2 μ M) made up in ethanol, and 4-OT (1 μ L, 2.9 μ g). When there is no further increase in the absorbance at 236 nm (indicating that **8** has been converted to **1**), a quantity (1 μ L, 0.5 μ g) of either 4-OD/VPH in 20 mM Tris-HCl buffer (containing 5 mM MnCl_2), pH 7.3, or 4-OD/E106QVPH in 20 mM NaH_2PO_4 buffer (containing 5 mM MgCl_2), pH 7.3, is added to the assay mixture and the decrease in absorbance at 236 nm is followed. VPH activity was monitored by following the rate of the decrease in absorbance at 265 nm ($\epsilon = 7850 \text{ M}^{-1} \text{ cm}^{-1}$) corresponding to the rate of the disappearance of **3**. The assay mixture consisted of 20 mM NaH_2PO_4 buffer, pH 7.3, made 5 mM in MgCl_2 (1 mL final volume) and 4-OD/VPH (1 μ L, 4.6 mg/mL). The assay was initiated by the addition of **3** (3 mL, 36 μ g) dissolved in ethanol.

^{13}C Isotope Effects. The ^{13}C isotope effects were determined by the protocol described by O'Leary (17). This technique uses the natural abundance of ^{13}C in the C-6 position of **1**. Both high-conversion (100% reaction) and low-conversion samples (20% reaction) were collected. The $^{12}\text{C}/^{13}\text{C}$ isotope ratios in the CO_2 produced in the reactions were determined for both samples. From these ratios, the relative rates for the reaction for ^{12}C vs ^{13}C , and thus the ^{13}C isotope effect, were calculated (18). The natural abundance method minimizes the errors introduced by atmospheric CO_2 contamination. Each reaction mixture for the low-conversion reaction was made up to a final volume of 40 mL and contained 20 mM Hepes buffer, pH 7.1, 10 M KOH (60 μ L) to compensate for the drop in the pH that occurs upon the addition of **8** as the free acid, and either 100 μ L of a 2 M MnCl_2 solution or 200 μ L of a 1 M MgCl_2 solution. The final metal ion concentration was 5 mM. Six reaction mixtures were set up. Three mixtures contained MnCl_2 and three contained MgCl_2 . The reaction mixtures were sparged overnight with CO_2 -free nitrogen. A solution of **8** (300 mg) dissolved in dimethyl sulfoxide was also sparged for 1 h with CO_2 -free nitrogen. Subsequently, **8** (39.5 mg) and 4-OT (50 μ L, 11 mg/mL) were added to the reaction mixtures. An aliquot (200 μ L) was removed and the absorbance at 236 nm was measured in order to determine the concentration of **1**. 4-OD/VPH (8 μ L, 4.16 mg/mL) was then added to the reaction mixture and the reaction progress was monitored by periodically removing aliquots and measuring the absorbance at 236 nm. When a reaction was \sim 20% complete (8–12 min), it was quenched with 0.2 mL of concentrated H_2SO_4 . Reaction mixtures for the high-conversion reactions were made up to a final volume of 40 mL and contained 20

Scheme 5



mM Hepes buffer, pH 7.1, 2 M MnCl₂ (100 μ L), and 10 M KOH (60 μ L). The three reaction mixtures were sparged overnight with CO₂-free nitrogen and **8** (9.5 mg) from the sparged stock solution described above, and then 4-OT (50 μ L, 11 mg/mL), and 4-OD/VPH (10 μ L, 4.16 mg/mL) were added. After incubation at room temperature overnight, the three reaction mixtures were quenched by the addition of 0.2 mL of concentrated H₂SO₄. The isotopic composition of the CO₂ was determined on an isotope-ratio mass spectrometer. All ratios were corrected for ¹⁷O according to Craig (19).

Determination of the Configuration of [5-D]3 Generated from 1 by 4-OD/E106QVPH. To a NMR tube was added a mixture of **8** (4 mg, 0.025 mmol) in dimethyl-*d*₆ sulfoxide and 100 mM Na₂DPO₄ (pD 9.3). The addition of **8** to the buffer adjusted the pD to 6.5. The substrate for 4-OD, **1**, was generated by the addition of 4-OT (0.06 μ g in 1 μ L), which had been previously exchanged into 20 mM NaD₂-PO₄ buffer (pD = 7.2). After 4 min, the major species in the mixture is **1** (**8**). 4-OD/E106QVPH (0.13 mg in 30 μ L) was added to the NMR tube and ¹H NMR spectra were acquired at timed intervals. The mutant complex had been previously exchanged into 20 mM NaD₂PO₄ buffer (pD = 7.2). A ¹H NMR spectrum of [5-D]**3** corresponded to a previously reported NMR spectrum (4). The observed coupling constant (*J* = 15 Hz) for the C-5 proton indicates a trans relationship to the C-4 proton (4).

Isolation of 3 Generated from 1 by 4-OD/E106QVPH. It has previously been reported that **3** and **5** can be generated in nearly equivalent amounts by the thermal decarboxylation of **8** (20). This procedure suffers from low and variable yields as well as the presence of **5**. A more reliable source of **3** was obtained by generating it enzymatically from 4-OD/E106QVPH complex as follows. To a suspension of **8** (0.2 g, 1.3 mmol) in 100 mM Na₂HPO₄ buffer (12 mL) was added a 42 μ L aliquot of a 1 M MgCl₂ solution in order to bring the final concentration of MgCl₂ to 3 mM. The pH of the suspension was adjusted to 6.5–7.2 by the addition of aliquots of 5 M NaOH solution. Adjustment of the pH results in the dissolution of **8**. The solution is then distributed in 0.6 mL portions into test tubes. A quantity of 4-OT (1 μ L of a 0.11 mg/mL solution) is added to each test tube and the mixture is allowed to incubate for 10 min. Subsequently, a quantity of 4-OD/E106QVPH (50 μ L of a 2.3 mg/mL solution) was added to each tube and the mixture was allowed to incubate for 15 min. After quenching of each individual reaction by the addition of 1 M HCl (300 μ L), the reactions were combined, the pH was adjusted to 1.0, and the samples were saturated with NaCl. The solution was extracted with ethyl acetate (3 \times), and the organic layers were pooled, dried over anhydrous Na₂SO₄, filtered, and evaporated to dryness at room temperature. The resulting solid was dissolved in CH₂Cl₂, and filtered through Whatman no. 1 filter paper in order to remove the residual **8**. The organic layer was

collected and evaporated to dryness at room temperature. The solid was dissolved in methanol, and the solution was passed through a nylon filter, collected, and evaporated to dryness at room temperature to yield **3** (typically 110–120 mg). The compound is stored at –20 $^{\circ}$ C. A ¹H NMR spectrum corresponded to the previously reported spectrum (20).

Assignment of the Stereochemistry at C-3 of 3-[D]4 Generated from 3 by 4-OD/VPH and by 4-OD/E106QVPH. The stereochemical analysis of 3-[D]**4**, generated by either the 4-OD/VPH- or the 4-OD/E106QVPH-catalyzed ketonization of **3** in D₂O, was performed by a literature procedure with the following modifications (Scheme 5) (21). The stereochemistry of the 4-OD/VPH-catalyzed reaction was reinvestigated as a control. The wild-type and mutant complexes were purified as described above and exchanged into 20 mM NaD₂PO₄ buffer (pD \sim 7.2) made up in D₂O. Metal ion was not added to the solution. Each reaction mixture consisted of enzyme (4-OD/VPH 80 μ g, 4-OD/E106QVPH 130 μ g) and **3** (4 mg) dissolved in DMSO-*d*₆ (30 μ L). A total of 15 reactions were carried out in 100 mM Na₂DPO₄ buffer (0.6 mL, pD = 9.3). The addition of **3** adjusted the pD to \sim 6.8. At 20, 50, and 90 s, a portion of a NaBH₄ solution (10 μ L of a 300 mg/mL solution) was added to each reaction mixture. The reaction mixtures were pooled and allowed to stand at room temperature overnight. Subsequently, the pH of the solution was adjusted to 8 and the product, **9** (4-OD/VPH 14 mg, 4-OD/E106QVPH 16 mg), was isolated by anion-exchange chromatography as described (21). A solution of **9** was subjected to ozonolysis as described. Most of the solvent was removed and the oily residue was dissolved in acetic acid (10 mL) and treated with 30% H₂O₂ (1 mL). After standing at room temperature for 2 days, most of the solvent was removed and the residue was dissolved in 20 mM sodium phosphate buffer (4 mL, pH 7.1). The pH was adjusted to 7.2, and catalase (40 μ L of a 4 mg/mL solution) was added in 5 μ L portions over a 15 min period. After 1 h, the bubbling stopped, the pH of the solution was adjusted to 8, and the diastereomeric [3-D]-D,L-malate (**10**) (4-OD/VPH 3.1 mg, 4-OD/E106QVPH 4.8 mg) was isolated by anion-exchange chromatography as described (21). Treatment of **10** with malic enzyme (to remove the 2S isomer of [3-D]malate) and purification of the product by anion-exchange chromatography, as described (21), afforded 1.3 mg (from 4-OD/VPH) or 1.7 mg (from 4-OD/E106QVPH) of the 2R isomer of [3-D]malate (**11**). (2R,3R)-[3-D]Malate (**11**) (from the 4-OD/E106QVPH-catalyzed reaction): ¹H NMR (CD₃OD, 500 MHz) δ 2.77 (\sim 0.5 H, br s, H3) and 4.45 (\sim 0.5 H, br q, H2). (2R,3S)-[3-D]Malate δ 2.61 (\sim 0.5 H, br d, *J*_{2,3} = 8 Hz, H3) and 4.46 (\sim 0.5 H, br q, H2).

RESULTS

Production, Expression, and Purification of the Recombinant Proteins. The gene for 4-OD was amplified from a subclone of the TOL plasmid pWW0, and the enzyme was expressed in *E. coli* strain BL21(DE3) and partially purified. It has previously been reported that the separately expressed 4-OD can be partially purified but that enzymatic activity cannot be recovered from a hydrophobic interaction column (2). Our attempts to purify 4-OD further by the addition of metal ion (Mg^{2+}) or glycerol were not successful. In our hands, the partially purified 4-OD rapidly loses activity when concentrated or stored.

The gene for VPH (*xylJ*) was amplified from cell extracts of *P. putida* mt-2, and the enzyme was expressed in *E. coli* strain BL21(DE3) as largely insoluble protein. This observation contrasts with an earlier report in which the separately expressed VPH was found to be soluble and readily purified (2). The *xylJ* gene was part of a large restriction fragment subcloned into an expression vector (designated pLV85) that contained the λ P_L promoter (3). Sequencing showed that the length of the gene in our expression system (261 codons) is 39 codons longer than the reported length of the *xylJ* gene (222 codons) (2), raising a question about the correct size of the gene. Initially, the insolubility of the product expressed by the longer gene suggested that the length of the gene is correct as reported. However, high levels of soluble VPH activity can be obtained when the longer gene is expressed as part of the 4-OD/VPH coexpression system (vide infra). Hence, the two sequences were examined more closely. In the reported sequence, the codon for the last amino acid (GCC) is followed by a stop codon (TGA). In our sequence, the GCC codon is followed by a codon for Leu (CTG), which, in turn, is followed by a codon for Lys (AAG). If the base in the first position of the CTG codon were deleted, a stop codon would be introduced and a truncated gene would be reported. Thus, our observation that VPH is largely insoluble may be due to its significantly higher expression in the pET system.

In view of the instability of 4-OD and the insolubility of VPH, a single plasmid was constructed that overexpressed both enzymes. The gene for 4-OD was modified at the 3' end to include two stop codons, a *Bam*HI restriction site, a ribosome binding site, the TATA box, and an *Nde*I restriction site. The purpose of two stop codons is to ensure that the translation of 4-OD stops before the translation of VPH begins. The *Bam*HI restriction site was introduced in order to verify the orientation of the 4-OD gene in the plasmid. The resulting PCR product was cloned into the pET24a-VPH plasmid at the 5' end of the gene for VPH. The sequence of both genes was confirmed by DNA sequencing. Subsequently, the plasmid was transformed into *E. coli* strain BL21(DE3) and expressed. The complex was purified to homogeneity (as assessed by SDS-PAGE) by a previously described procedure (2). Typically, this procedure yields ~10 mg of pure 4-OD/VPH complex/L of cell culture.

Finally, Glu-106 of VPH was changed to glutamine, and the resulting E106Q mutant was expressed in *E. coli* strain BL21(DE3) as a complex with 4-OD. The sequence of the mutant was confirmed by DNA sequencing. The 4-OD/E106QVPH complex was purified following the procedure used for the purification of the 4-OD/VPH complex (2).

Table 1: Primary ^{13}C Kinetic Isotope Effects for the Enzymatic Decarboxylation of **1**

experiment	metal	$\delta^{13}\text{C}$	f^a	$^{13}(\text{V/K})$
partial conversion	Mn^{2+}	-64.46	0.14	1.038
		-66.05	0.16	1.040
		-65.27	0.14	1.039
partial conversion	Mg^{2+}	-61.40	0.18	1.035
		-64.47	0.20	1.040
100% conversion	Mn^{2+}	-31.71	1.0	1.038 ± 0.02^b
		-30.99	1.0	
		-31.30	1.0	

^a The largest error is in the f value. As a result, the measured values of $^{13}(\text{V/K})$ are identical within experimental error and independent of Mn^{2+} or Mg^{2+} . The average value for all determinations is reported.

^b Average value for all determinations.

Typically, 10 mg of protein (>90% homogeneous) is obtained/L of culture.

Kinetic Properties of 4-OD in the 4-OD/VPH Complex and in the 4-OD/E106QVPH Complex. The rate of decarboxylation of **1** by the 4-OD/VPH complex and the 4-OD/E106QVPH complex was measured by following the loss in absorbance at 236 nm. For the 4-OD/VPH complex, the value of K_m is $6.6 \pm 0.6 \mu\text{M}$ and the value of k_{cat} is $68 \pm 2 \text{ s}^{-1}$. This results in a $k_{\text{cat}}/K_m = 1.0 \times 10^7 \text{ M}^{-1} \text{ s}^{-1}$. For the 4-OD/E106QVPH complex, the value of K_m is $13 \pm 1 \mu\text{M}$ and the value of k_{cat} is $67 \pm 2 \text{ s}^{-1}$. This results in a $k_{\text{cat}}/K_m = 5.1 \times 10^6 \text{ M}^{-1} \text{ s}^{-1}$. Thus, the mutation in VPH has not significantly altered the steady-state kinetic parameters of 4-OD.

^{13}C Isotope Effects. The carbon isotope effect on the decarboxylation of **1** was measured as follows. The ^{13}C content of the CO_2 generated in the partial conversion of substrate to product in the presence of Mn^{2+} and Mg^{2+} were determined and compared to the isotopic content of the substrate. The latter was assessed by analysis of the CO_2 generated in the complete (i.e., 100%) conversion of substrate to product. The data for the ^{13}C isotope effects of the enzymatic decarboxylation of **1** are summarized in Table 1. No significant difference is observed whether Mg^{2+} or Mn^{2+} is used as the divalent metal ion. The average ^{13}C isotope effect is 1.038 ± 0.002 . Thus, the isotope effect is independent of the metal ion.

Determination of the Configuration of [5-D]3 Generated from **1 by 4-OD/E106QVPH.** As part of the characterization of 4-OD in the 4-OD/E106QVPH mutant, the configuration of the isomer of [5-D]3 (4E vs 4Z) generated by the decarboxylation of [5-D]1 was established by ^1H NMR analysis. The coupling constants between the two protons at C-5 of **3** and the proton at C-4 have been assigned (4). In D_2O , [5-D]3 was generated by the incubation of **8**, 4-OT, and 4-OD/E106QVPH. Subsequent analysis of [5-D]3 clearly showed that the remaining proton at C-5 is trans to the proton at C-4, indicating that the 4E isomer had been produced. Likewise, the 4-OD/VPH complex yields the 4E isomer of [5-D]3. Thus, the mutation in VPH has not altered the configuration of [5-D]3.

Assignment of the Stereochemistry at C-3 of 3-[D]4 Generated from **3 by 4-OD/VPH and by 4-OD/E106QVPH.** In separate reactions, **3** was converted to [3-D]4 in D_2O by either the wild-type or the mutant complex. Subsequently, [3-D]4 was isolated and processed to the 2R isomer of [3-D]-

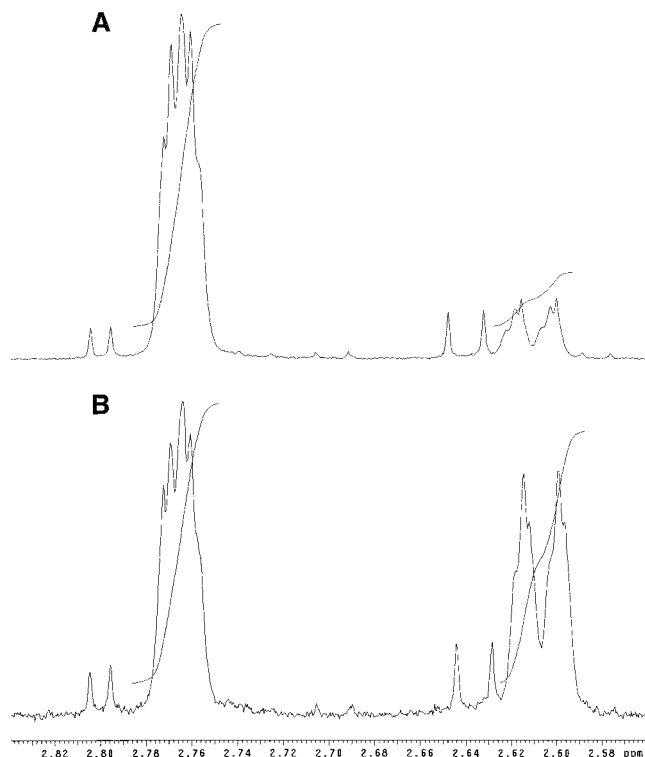


FIGURE 1: ^1H NMR (500 MHz, CD_3OD) spectrum of $(2R)$ -[3-D]-malate obtained from the chemical and enzymatic conversion of [3-D]**4** generated by the incubation of **3** with (A) the 4-OD/VPH complex and (B) the 4-OD/E106QVPH mutant complex in D_2O . The signal at 2.77 ppm corresponds to the $(2R,3R)$ -isomer and the signal at 2.61 ppm corresponds to the $(2R,3S)$ -isomer. The other signals in the spectrum correspond to the fully protio malate and other impurities.

malate (**11**) by a previously described sequence of reactions (Scheme 5) (4, 21). The malate recovered in both reactions was analyzed by ^1H NMR spectroscopy.

In CD_3OD , each diastereotopic proton at C-3 of the fully protio malate appears as a doublet as 2.61 and 2.77 (21, 22). Stereospecific incorporation of a deuterium at C-3 results in the loss of one signal and the collapse of the remaining signal into a broadened doublet (23). The resonances for $(2R)$ -[3-D]malate have been assigned by the reaction of maleic acid with maleate hydratase in D_2O (22). When the reaction is performed in D_2O , $(2R,3R)$ -[3-D]malate is obtained and the resulting ^1H NMR spectrum in CD_3OD shows the loss of an upfield signal (2.61 ppm) and the presence of a downfield doublet (2.77 ppm) (21, 22).

The stereochemistry of the 4-OD/VPH-catalyzed conversion of **3** to **4** was reinvestigated as a control. The ^1H NMR spectrum of the $(2R)$ -[3-D]malate, isolated after the conversion of [3-D]**4** to **11**, is shown in Figure 1A. One signal is centered at 2.61 ppm and the other signal is centered at 2.77 ppm. The integral of the signal at 2.77 ppm, assigned to the $(2R,3R)$ -isomer, is 6.2-fold greater than that of the corresponding integral for the $(2R,3S)$ -isomer observed at 2.61 ppm. Thus, the reaction is highly stereoselective as has been previously reported (4), and the stereochemistry at C-3 of [3-D]malate indicates that the stereochemistry at C-3 of **4** is *S*. The priority numbering at C-3 changes because there is a double bond instead of a carboxylate group at C-4 (Scheme 5).

The ^1H NMR spectrum of the $(2R)$ -[3-D]malate isolated after the conversion of [3-D]**4** to **11** is shown in Figure 1B.

The spectrum shows the same signals centered at 2.61 and at 2.77 ppm. However, the integrals for these two signals are comparable, which indicates that a racemic mixture of $(2R,3R)$ -[3-D]malate and $(2R,3S)$ -[3-D]malate has been isolated. Thus, the conversion of **3** to **4** in the 4-OD/E106QVPH-catalyzed reaction is stereorandom, indicating that the reaction is a nonenzymatic process.

DISCUSSION

The 4-OD/VPH complex catalyzes an interesting sequence of reactions and raises a number of mechanistic and structural questions. Among these questions are the mechanics of how each reaction is carried out, whether there are independent active sites, the extent of communication between these active sites (i.e., channeling) if any, and the structure and metabolic purpose of this complex. Studies to address these questions have been hampered by insufficient quantities of enzymes, uncertainty about the intermediates involved in the transformation of **1** to **2**, and the fact that the two enzymes exist as a complex. The results of this investigation resolve these problems and provide new insights into the two reactions and together facilitate future mechanistic and structural studies.

The genes for 4-OD and VPH have previously been cloned as part of separate restriction fragments into *E. coli* under control of the λ P_L promoter and expressed at low levels (2). Presumably, higher expression levels were not obtained because the location of the coding sequence for the genes was unknown so that the correct alignment with the ribosome-binding site might not have been achieved. Thus, our strategy relied on placing the gene in proper juxtaposition with an efficient promoter and the ribosome-binding site. While this strategy did not lead to the separate production of either 4-OD or VPH as stable, soluble proteins, it did allow for the coexpression and, ultimately, purification of both proteins as a complex.

In view of the fact that 4-OD and VPH could not be expressed separately, an alternate strategy was pursued in which each enzyme of the complex would be inactivated by mutagenesis of critical residues identified through sequence analyses. Thus far, this strategy has resulted in the construction of a complex having only 4-OD activity. Potential candidates for mutagenesis were determined by using a previously reported comparison of VPH with 11 other sequences that code for hydratases in various degradative pathways (6, 7). This analysis revealed the presence of five identically conserved aspartate residues (Asp-78, Asp-154, Asp-158, Asp-178, and Asp-254) and three identically conserved glutamate residues (Glu-106, Glu-108, and Glu-139). It has been suggested that many of these residues may be metal binding ligands while others may be involved in catalysis (6,7). In an attempt to identify roles for these residues, the aspartate residues (with the exception of Asp-78) of 2-oxohept-4-ene-1,7-dioate (OHED) hydratase, the corresponding hydratase to VPH found in the homoproteocatechuate metafission pathway (14), were changed, individually, to asparagine residues.² Likewise, the glutamate residues of OHED hydratase were mutated, individually, to glutamine residues. All of the mutants were found to be

² Q. Kong, E. A. Burks, C. P. Whitman (1998) unpublished results.

insoluble with the exception of the E106Q mutant, which had no OHED hydratase activity. For these reasons, Glu-106 in the VPH sequence was changed to a glutamine, and the resulting mutant was expressed as a complex with 4-OD.

A kinetic analysis of the resulting 4-OD/E106QVPH mutant complex clearly shows that the complex retained full 4-OD activity (as assessed by its kinetic parameters) but had no VPH activity. In addition, stereochemical studies confirm that the mutant complex generates the 4*E* isomer of [5-D]**3**, as does the wild-type complex. Thus, the mutation in VPH does not affect the kinetic parameters or the stereochemistry of the 4-OD-catalyzed reaction, suggesting that the active sites of 4-OD and VPH are largely independent.

These results also implicate **3** as the product of the 4-OD reaction and as the substrate for VPH. This observation is consistent with two previous studies on VPH (2, 7). Harayama et al. (2) reported that freshly prepared solutions of **3** were processed by VPH faster than aged solutions. However, the isomeric composition of the aged solutions was not determined, and depending on the age of the solution, a large portion of these solutions might have been (3*E*)-**5**, an isomer not processed by VPH (4,7). A more recent and rigorous kinetic analysis showed that **3** is processed by a related VPH from *Escherichia coli* without a lag time (7). The absence of a lag time suggested that **3** (and not **4**) is the substrate for VPH.

These studies further indicate that VPH is responsible for the highly stereoselective ketonization of **3** in the 4-OD/VPH complex and that Glu-106 is the likely residue involved in this transformation. Moreover, the observation that Glu-106 is essential for VPH activity suggests that it might be a catalytic residue. One notable example of an enzyme-catalyzed hydration reaction mediated by a glutamate residue is that of enoyl-CoA hydratase (24–26). The enzyme catalyzes the hydration of α,β -unsaturated fatty acid CoA thioesters (25). Kinetic, site-directed mutagenesis, and crystallographic studies implicate two glutamate residues (Glu-144 and Glu-164) in the mechanism (24–26). It is also possible that the lack of hydratase activity is due to a structural perturbation or to the enzyme's inability to bind metal ion. The role of Glu-106 in the mechanism of VPH is currently under investigation.

The combination of the kinetic and stereochemical results suggests a straightforward scenario for the transformation of **1** to **2**. First, 4-OD catalyzes the decarboxylation of **1** to generate **3**. Subsequently, VPH catalyzes the ketonization of **3** to **5**. This step is followed by the Michael addition of water to **5**, resulting in **2**. This scenario does not account for the highly stereoselective VPH-catalyzed ketonization of **3** to **4** and it is not yet clear what role such a step would play. A possible explanation may be related to the observation that **3** and **4** rapidly interconvert in solution. The enzyme-catalyzed interconversion of **3** and **4** may have evolved in order to prevent the nonenzymatic interconversion from becoming the rate-limiting step of the overall reaction.

The mechanism of the 4-OD reaction was also examined by measuring the ^{13}C isotope effect on the reaction. The rather large ($\sim 4\%$) ^{13}C isotope effect found on the reaction indicates that that carbon–carbon bond cleavage (i.e., decarboxylation) is rate-limiting or nearly rate-limiting. This conclusion is further supported by the observation that the ketonization of **3** is not catalyzed by 4-OD, thereby eliminat-

ing one potentially rate-limiting step in the reaction. The observed isotope effect is also slightly smaller than the intrinsic isotope effects ($\sim 5\%$) measured for several decarboxylation reactions including those of malic enzyme (18, 27–29), isocitrate dehydrogenase (30), and 6-phosphogluconate dehydrogenase (31). Although the intrinsic isotope effect has not yet been measured for the 4-OD reaction, it can be tentatively concluded, on the basis of these examples, that the intrinsic isotope effect for 4-OD will be similar and that the reaction has a late transition state.³ The identity of the isotope effects with either divalent metal ion (Table 1) suggests that the transition state is independent of the metal ion. Finally, the combination of these observations suggests a mechanism for 4-OD in which the metal ion chelates to the 1-carboxylate oxygen and the 2-keto carbonyl group (32). This arrangement polarizes the 2-keto carbonyl group, decreases the electron density at the scissile carbon-5 carbon-6 bond, and stabilizes the enolate (32).

The metal-dependent decarboxylation of **1** is reminiscent of the metal-dependent decarboxylation of **6**. As noted earlier, the sole difference between the two substrates is the double bond in **1** conjugated with the carbonyl group. One obvious question raised by this structural difference is whether the double bond changes the mechanism. The metal-dependent decarboxylations of oxalacetate by malic enzyme, pyruvate kinase, and oxalacetate decarboxylase have been extensively studied (18, 27–29, 33, 34). In addition, the nonenzymatic metal-dependent decarboxylation of oxalacetate has been examined (32). The ^{13}C isotope effect measured for these reactions ranged from $\sim 2\%$ to 5% , indicative of a late transition state (18, 27–29, 33, 34). Moreover, on the basis of these studies, it was proposed that the metal ion forms a complex with the α -keto acid portion and acts as an electron sink to stabilize the enolate intermediate (32). Thus, with regard to the mechanism of decarboxylation, 4-OD proceeds in a manner similar to that of OAD.

ACKNOWLEDGMENT

We thank Steve D. Sorey, Department of Chemistry, University of Texas at Austin, for his help in obtaining the 500 MHz proton NMR spectra.

SUPPORTING INFORMATION AVAILABLE

Description of the construction of the pET24a-4OD and pET24a-VPH plasmids, the overexpression of 4-OD and VPH, and the partial purification of 4-OD. This material is available free of charge via the Internet at <http://pubs.acs.org>.

REFERENCES

1. Collinsworth, W. L., Chapman, P. J., and Dagley, S. (1973) *J. Bacteriol.* **113**, 922–931.
2. Harayama, S., Rekik, M., Ngai, K.-L., and Ornston, L. N. (1989) *J. Bacteriol.* **171**, 6251–6258.
3. Harayama, S., Lehrbach, P. R., and Timmis, K. (1984) *J. Bacteriol.* **160**, 251–255.
4. Lian, H., and Whitman, C. P. (1994) *J. Am. Chem. Soc.* **116**, 10403–10411.

³ The data suggest that there may be a step prior to decarboxylation that also partially limits the overall reaction under *V/K* conditions. Nonetheless, given the large ^{13}C isotope effect, the transition state for carbon–carbon bond cleavage is late.

5. O'Leary, M. H. (1992) in *The Enzymes* (Sigman, D. S., Ed.) Vol. 20, pp 235–269, Academic Press, San Diego, CA.
6. Kim, S., Kweon, O.-K., Kim, Y., Kim, C.-K., Lee, K.-S., and Kim, Y.-C. (1997) *Biochem. Biophys. Res. Commun.* 238, 56–60.
7. Pollard, J. R., and Bugg, T. D. H. (1998) *Eur. J. Biochem.* 251, 98–106.
8. Whitman, C. P., Aird, B. A., Gillespie, W. R., and Stolowich, N. J. (1991) *J. Am. Chem. Soc.* 113, 3154–3162.
9. Czerwinski, R. M., Johnson, W. H., Jr., Whitman, C. P., Harris, T. K., Abeygunawardana, C., and Mildvan, A. S. (1997) *Biochemistry* 36, 14551–14560.
10. Sambrook, J., Fritsch, E. F., and Maniatis, T. (1989) *Molecular Cloning: A Laboratory Manual*, Cold Spring Harbor Laboratory, Cold Spring Harbor, NY.
11. Goode, B. L., and Feinstein, S. C. (1992) *BioTechniques* 12, 374–375.
12. Laemmli, U. K. (1970) *Nature* 227, 680–685.
13. Khokhlatchev, A. Xu, S., English, J., Wu, P., Schaefer, E., and Cobb, M. H. (1997) *J. Biol. Chem.* 272, 11057–11062.
14. Burks, E. A., Johnson, W. H., Jr., and Whitman, C. P. (1998) *J. Am. Chem. Soc.* 120, 7665–7675.
15. Schillberg, S., Schumann, D., and Fischer, R. (1997) *Bio-Techniques* 23, 212–216.
16. Ho, S. N., Hunt, H. D., Horton, R. M., Pullen, J. K., and Pease, L. R. (1989) *Gene* 77, 51–59.
17. O'Leary, M. H. (1980) *Methods Enzymol.* 64, 83–104.
18. Hermes, J. D., Roeske, C. A., O'Leary, M. H., and Cleland, W. W. (1982) *Biochemistry* 21, 5106–5114.
19. Craig, N. (1957) *Geochim. Cosmochim. Acta* 12, 133–140.
20. Lian, H., and Whitman, C. P. (1993) *J. Am. Chem. Soc.* 115, 7978–7984.
21. Harris, T. K., Czerwinski, R. M., Johnson, W. H., Jr., Legler, P. M., Abeygunawardana, C., Massiah, M. A., Stivers, J. T., Whitman, C. P., and Mildvan, A. S. (1999) *Biochemistry* 38, 12343–12357.
22. Gawron, O., Glaid, A. J., and Fondy, T. P. (1961) *J. Am. Chem. Soc.* 83, 3634–3640.
23. Englund, S., Britten, J. S., and Listowsky, I. (1967) *J. Biol. Chem.* 242, 2255–2259.
24. Engel, C. K., Mathieu, M., Zeelen, J. P., Hiltunen, J. K., and Wierenga, R. K. (1996) *EMBO J.* 15, 5135–5145.
25. He, X.-Y., and Yang, S.-Y (1997) *Biochemistry* 36, 11044–11049.
26. Hofstein, H. A., Feng, Y., Anderson, V. E., and Tonge, P. J. (1999) *Biochemistry* 38, 9508–9516.
27. Park, S.-H., Harris, B. G., and Cook, P. F. (1986) *Biochemistry* 25, 3752–3759.
28. Grissom, C. B., and Cleland, W. W. (1988) *Biochemistry* 27, 2927–2934.
29. Karsten, W. E., and Cook, P. F. (1994) *Biochemistry* 33, 2096–2103.
30. Grissom, C. B., and Cleland, W. W. (1988) *Biochemistry* 27, 2934–2943.
31. Hwang, C.-C., Berdis, A. J., Karsten, W. E., Cleland, W. W., and Cook, P. F. (1988) *Biochemistry* 36, 12596–12602.
32. Grissom, C. B., and Cleland, W. W. (1986) *J. Am. Chem. Soc.* 108, 5582–5583.
33. Kiick, D. M., and Cleland, W. W. (1989) *Arch. Biochem. Biophys.* 270, 647–654.
34. Waldrop, G. L., Braxton, B. F., Urbauer, J. L., Cleland, W. W., and Kiick, D. M. (1994) *Biochemistry* 33, 5262–5267.

BI9918902